JACS
JOURNAL OF THE AMERICAN CHEMICAL SOCIETY

Article

pubs.acs.org/JACS

Two- and Three-Electron Oxidation of Single-Site Vanadium Centers at Surfaces by Ligand Design

Daniel Skomski, Christopher D. Tempas, Brian J. Cook, Alexander V. Polezhaev, Kevin A. Smith, Kenneth G. Caulton,* and Steven L. Tait*

Department of Chemistry, Indiana University, 800 East Kirkwood Avenue, Bloomington, Indiana 47405, United States

Supporting Information

ABSTRACT: Rational, systematic tuning of single-site metal centers on surfaces offers a new approach to increase selectivity in heterogeneous catalysis reactions. Although such metal centers of uniform oxidation states have been achieved, the ability to control their oxidation states through the use of carefully designed ligands had not been shown. To this end, tetrazine ligands functionalized by two pyridinyl or pyrimidinyl substituents were deposited, along with vanadium metal, on the Au(100) surface. The greater oxidizing power of the bis-pyrimidinyltetrazine facilitates the on-surface redox formation of V^{3+}, compared to V^{2+} when paired with the bis-pyridinyltetrazine, as determined by X-ray photoelectron spectroscopy. This demonstrates the ability to control metal oxidation states in surface coordination architectures by altering the redox properties of organic ligands. The metal−ligand complexes take the form of one-dimensional polymeric chains, resolved by scanning tunneling microscopy. The chain structures in the first layer are very uniform and are based on the same quasi-square-planar coordination geometry around single-site V with either ligand. Formation of a different, dimer structure is observed in the early stages of the second layer formation. These systems offer new opportunities in controlling the oxidation state of single-site transition metal atoms at a surface for new advances in heterogeneous catalysts.

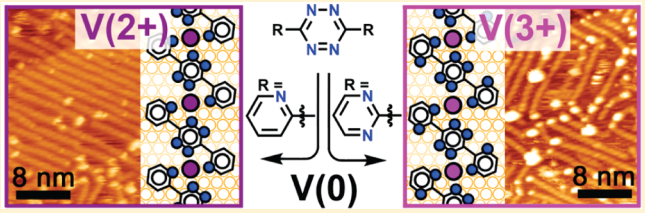

INTRODUCTION

High selectivity in next-generation catalysts requires structural as well as chemical control of single-site metal centers at surfaces in order to maintain uniform and specific chemistry at all active sites. On-surface metal−ligand coordination is a promising strategy to achieve structurally and chemically well-defined metal centers,[1] while also providing an opportunity for bifunctional character through intimate contact with a surface. A key challenge in the on-surface assembly of metal−ligand coordination networks is to develop a ligand library to access and program any one of a variety of metal oxidation states, which is important for tuning chemical selectivity in heterogeneous catalysis.[2,3] Several prior examples of on-surface metal−ligand coordination involved diatomic elimination (e.g., H_2), as in porphyrin[4,5] and terephthalic acid[6] metalation with surface-supported elemental metal, such that the resultant complexed metals adopted a +2 oxidation state. In our recent studies of direct donation of electrons into a redox-active tetrazine[7] or ketone-functionalized phenanthroline[8] a +2 metal oxidation state was achieved without diatomic elimination for platinum, chromium, and iron. This demonstrated on-surface redox chemistry to produce structurally uniform single site metal(2+) centers which are also uniform in oxidation state. Here, we demonstrate the implementation of redox non-innocent ligands to achieve the essential ability to change the metal oxidation state by rational molecular design of redox-active subunits and thus achieve higher oxidation states than +2.

We were interested in demonstrating a controlled variation in the ligand field to access a +2 or a +3 oxidation state in related metal species, while leaving the axial site of the metal unoccupied and thereby available for subsequent binding. Here, we present examples of the oxidation of metallic (i.e., charge-neutral) vanadium to the +2 or +3 oxidation state by coordination to bis-pyridinyltetrazine or bis-pyrimidinyltetrazine, respectively, on the reconstructed Au(100) surface.

Tetrazines, which possess a low-lying π^* orbital due to their heavy sp^2 nitrogen loading, are known to act as an oxidant to an electron rich metal.[9] We previously illustrated the utility of bis-pyridinyltetrazine (**1**, Scheme 1) to ligate and oxidize Pt metal atoms to the +2 oxidation state on a gold surface.[7] Oxidation to the common Pt +4 oxidation state was not observed. To achieve higher oxidation states, we thus considered V, which has applications in heterogeneous catalysis,[2,10] including for selective alkane oxidation,[11] and in homogeneous catalysis[12,13] and is a stronger reducing agent than Pt. Also, V is known to be able to access a greater variety of oxidation states (−3 to +5)[14] although none of these have been previously characterized in an on-surface environment for metal−ligand systems; only various VO_x surfaces have been characterized in surface studies.[15]

Received: April 20, 2015
Published: June 1, 2015

DOI: 10.1021/jacs.5b03706
J. Am. Chem. Soc. 2015, 137, 7898−7902

Scheme 1. Bis-pyridinyltetrazine (1) and Bis-pyrimidinyltetrazine (2) Ligands Used in This Study and the $(1^{2-}\text{-}V^{2+})_n$ and $(2^{3-}\text{-}V^{3+})_n$ Polymers That Result from Their Redox Assembly on the Au(100) Surface[a]

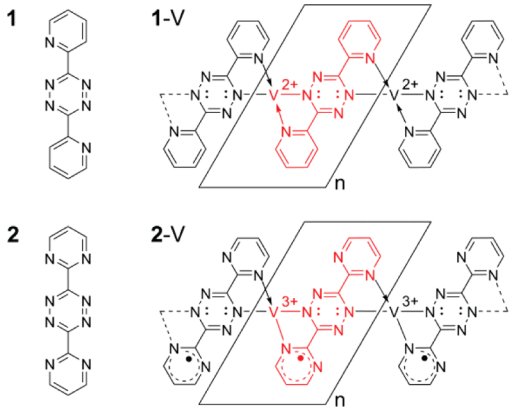

[a]One repeat unit is shown in red for each polymer. One of the three electrons transferred in forming V^{3+} is shown in one pyrimidinyl ring, but is in fact delocalized equally (second resonance form) into the second pyrimidinyl in each monomer unit.

EXPERIMENTAL SECTION

The experiments were conducted in a pristine ultrahigh vacuum (UHV) system (<5 × 10^{-10} Torr). The system is equipped with both scanning tunneling microscopy (STM) and non-contact atomic force microscopy (NC-AFM) (SPM UHV 750, RHK Technologies) as well as X-ray photoelectron spectroscopy (XPS) (electron energy analyzer PHOIBOS 150 and Mg/Al dual anode X-ray source XR-50, SPECS GmbH). The interconnected vacuum chambers allow for STM, NC-AFM, and XPS on the same samples.

STM imaging and XPS acquisition were conducted at room temperature. The well-characterized, (3×3) structure of terephthalic acid on the copper (100) surface[6,16,17] was used to calibrate the SPM instrument. Sharp tungsten STM tips were fabricated with electrochemical etching. Bias voltages of 1.0−1.2 V and set point currents from 0.2 to 0.4 nA were generally used for the STM imaging. SPM image analysis was conducted using the WSxM software.[18]

The reconstructed gold (100) single-crystal surface was cleaned before each experiment by 3−4 cycles of argon ion sputtering, with the sample held at 200 °C, and thermal annealing to 550 °C. Under these conditions, the Au(100) surface spontaneously reconstructs to a quasi-hexagonal $c(26\times68)$ reconstruction.[19,20] Bis-pyridinyltetrazine (**1**, 96%) was purchased from Sigma-Aldrich. Bis-pyrimidyltetrazine (**2**) was synthesized by a coupling reaction between 2-pyrimidinecarbonitrile and hydrazine in acidic media followed by oxidation of the dihydrotetrazine intermediate, in a procedure adapted from Kaim and Fees.[21] Ligands **1** and **2** were degassed for 18 and 2 h, respectively, in a quartz crucible in UHV at temperatures of 90−100 and 105 °C, respectively. They were vapor deposited from a Knudsen-type evaporator in UHV at sublimation temperatures of 115 and 125 °C, respectively. Vanadium (99.8% pure rod, Goodfellow) was vapor deposited using an electron beam evaporator (QUAD-EV-S Mini e-beam Evaporator, Mantis Deposition Ltd.).

RESULTS AND DISCUSSION

The surface structures are studied here with STM and XPS in UHV to gain insight into the on-surface redox chemistry leading to formation of the adsorbate structure. The redox assembly occurs regardless of the deposition order of the metal and the ligand. Control experiments conducted with deposition of only V or with deposition of only ligand were conducted and are reported in the Supporting Information (SI). In either case, no evidence for redox activity is observed unless both components are present. Further control studies that vary the relative ratio of V to **1** or **2** show that the redox reaction is nearly quantitative if the surface coverage is below ∼0.5 ML to allow sufficient room for mixing.

XPS measurements of the V $2p_{3/2}$ photoelectron peak allow direct characterization of the core level electron binding energies, which will vary with the oxidation state of V and can thus be used to probe the effect of the redox reaction with ligands **1** or **2** on the V charge state. The V $2p_{1/2}$ peak is not shown in Figure 1a−c for clarity of presentation, but it is shown

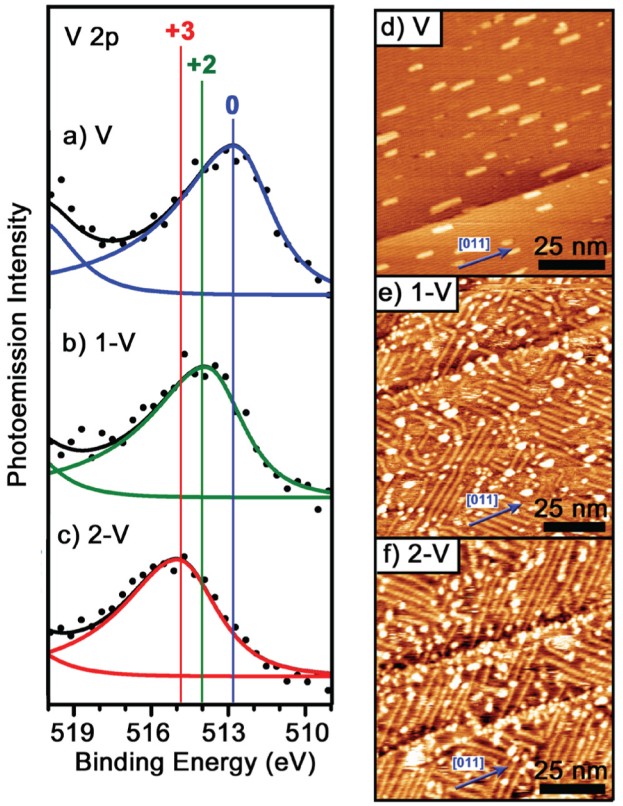

Figure 1. (a−c) Vanadium $2p_{3/2}$ XP spectra and (d−f) STM images for (a,d) V, (b,e) **1**-V, and (c,f) **2**-V on the reconstructed Au(100) surface after annealing at 170−200 °C. In each of **1**-V and **2**-V, the V:ligand ratio is 1, and the ligand was deposited first and V metal second with sub-monolayer quantities of each. (b) Oxidation of V by ligand **1** is evidenced by the 1.1 eV shift to higher binding energy, consistent with V(II)-phthalocyanine on Ag(111)[24] and V(II) oxide.[15] (c) Oxidation of V by ligand **2** is evidenced by the 1.9 eV shift to higher binding energy and referenced to V(III)-N complexes.[25,26] (d) Wide-scan STM image of the V islands (bright nanoparticles) which are elongated along the rows of the Au reconstruction. (e,f) The metal−ligand chains are predominantly oriented at a 45° angle from the direction of the Au reconstruction. The entire V 2p spectra (including the $2p_{1/2}$ photoelectron peak) are shown in Figure S6.

in Figure S6 in the SI. Each of the V 2p fit components discussed here is a pair of components for the $2p_{1/2}$ and $2p_{3/2}$ with constrained relative peak separation, ΔBE, and area ratios, as discussed in the SI. The V $2p_{3/2}$ BE for a sub-monolayer quantity of pure V (no ligand) on the reconstructed Au(100) surface (Figure 1a; 512.7 eV) matches the value reported for bulk V metal (charge-neutral) (512.7 eV[22]) showing that final state effects in the V/Au surface environment are comparable those at the V surface, as expected.[23] Ligand **1** induces a 1.1 eV chemical shift of V 2p to higher BE (Figure 1b, 513.8 eV),

DOI: 10.1021/jacs.5b03706
J. Am. Chem. Soc. 2015, 137, 7898−7902

consistent with oxidation of V. This shift is comparable to that expected from comparison to V(II)-phthalocyanine on Ag(111)[24] or vanadium(II) oxide.[15] Ligand **2** induces a 1.9 eV chemical shift to higher BE (Figure 1c, 514.7 eV) indicating still greater oxidation than by **1**. Each of these data sets is fit well by a single component, indicating a quantitative yield of the on-surface oxidation of the V metal; i.e., XPS does not resolve residual charge-neutral V (experimental details for achieving complete oxidation are provided in the SI). The V binding energy in **2**-V matches the +3 oxidation state in V(III)-N complexes, such as VN[25] and V-hydrazide[26] (514.4−515.0 eV). Since pyrimidinyl is an electron-withdrawing group on the tetrazine (lowers the π^* energy) **2** is more easily reduced than **1**, and **2** will delocalize electrons from the tetrazine into both pyrimidinyl rings creating amide nitrogen atoms there (see Scheme 1). Consequently, the pyrimidinyl nitrogen atoms also become stronger donors in coordinate covalent bonds to the oxidized vanadium in the 1D polymer structure. The pyridinyl substituents in **1** are less effective electron acceptors than the pyrimidinyls in **2**; thus, the V 2p binding energy of **1**-V falls between the charge-neutral V metal and **2**-V and is assigned to the +2 chemical state.[15,27] The model presented in Scheme 1 assumes that all charge is maintained in the 2D plane, but there is certainly some charge transfer to/from the surface and the induced charge in the metallic surface may play a significant role in stabilizing the polymer chains.[28]

XPS analysis of the N 1s core levels of the ligands in the metal−ligand complexes shows a significant spectroscopic change (Figure 2), indicating an alteration in chemical state upon redox assembly. Corresponding C 1s spectra are presented in the SI (Figure S7). Quantitative analysis of the XPS intensities for V and N yield a 1:1 V:ligand stoichiometry, as depicted in Scheme 1. A monolayer of **1** (no V present, Figure 2a) shows two N 1s features at energies of 399.8 and 398.3 eV, which correspond to the tetrazine and pyridinyl N, respectively, and appear in the XP spectra in the 2:1 area ratio anticipated from the molecular structure. Upon redox reaction with V, we anticipate three distinct N chemical states in a 1:1:1 ratio (see Scheme 1, **1**-V). Indeed, the resulting XP spectrum (Figure 2c) appears as a broad feature (significantly larger width indicates a convolution of multiple components), which is fit very well with three components of the same peak width as for neutral **1** (400.0, 399.1, and 398.3 eV), and is also consistent with the previously studied divalent Pt surface complex.[7] While metal-free ligand **1** thermally desorbs from the surface at 170 °C (Figure 2b), the **1**-V polymer is stable against thermal desorption up to at least 200 °C (Figure 2d), indicating a relatively strong metal−ligand coordination bond.

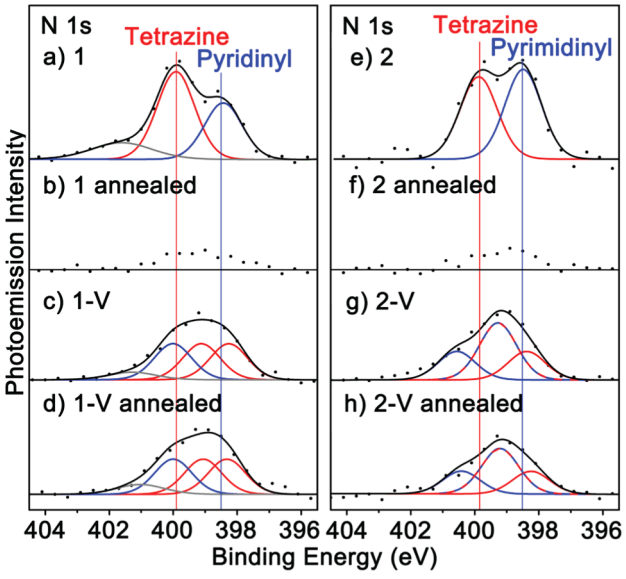

Figure 2. Nitrogen 1s XPS photoelectron peaks for **1** and **2** on the reconstructed Au(100) surface, in their pure form and after addition of V, before and after annealing at 170−200 °C for 10 min. (a,e) Each ligand in its pure form (no V present) exhibits two N 1s features, corresponding to the two species of N in each molecule at the anticipated area ratios. (b,f) Each of these desorbs from the surface by thermal annealing in the absence of V. (c,g) After on-surface complexation with V, an additional component is observed in each spectrum consistent with distinct N states in the polymer complexes. (d,h) The bonding within the complexes resists thermal desorption. The broad features at high BE (colored gray in parts a−d) are shake-up peaks.

A monolayer of **2** (Figure 2e) shows two N 1s XP spectral features, which correspond to tetrazine and pyrimidine N in a 1:1 area ratio (399.9 and 398.5 eV). Molecules of **2** (without V) desorb from the surface with thermal annealing at 200 °C (Figure 2f). Upon redox reaction with V, the **2**-V spectrum (Figure 2g) can be described by tetrazine reduction and partial reduction of the pyrimidinyl rings. The charge accepted by the tetrazine ligand is concentrated on the two N atoms that bind V(III), with a resultant degeneracy of the N 1s binding energies of the tetrazine N atoms that is analogous to the case of **1**-V. The charge accepted by the pyrimidinyl substituents is delocalized over both rings, but the greatest resonance contribution is expected from the structure that has charge concentrated on the N atoms binding V(III), thereby splitting the pyrimidinyl N 1s signal. While four unique N chemical states are anticipated from the model in Scheme 1, the data are well fit by three components with the same peak width as neutral **2** in a 1:2:1 ratio (400.4, 399.2, and 398.2 eV); i.e., two of the expected four chemical states have a similar BE. The N 1s XP spectrum of **2**-V presents further evidence for the change in the redox state of the ligand and is consistent with the analysis of the **1**-V spectrum. The resultant **2**-V is stable against thermal annealing (Figure 2h) at 200 °C (the desorption temperature of metal-free **2** ligand). A complete list of XPS peak positions from this study and comparison to relevant reference literature are provided in the SI.

High-resolution STM images indicate the formation of 1D metal−ligand polymer chains when V is mixed with either **1** (Figures 1e and 3a,c) or **2** (Figures 1f and 3b) on the Au(100) surface. The structures of the metal−organic 1D polymers for each of the two ligands in this study are nearly identical. Each has a morphology that is markedly different from the rectangular 2D islands of pure V (without ligand) on the same surface (Figure 1d) or from either the 2D domains of metal-free **1** molecules[7] or the mobile and unresolved sub-monolayer phase of metal-free **2** molecules (Figure S4). Zoom-in STM images of the 1D polymers (Figure 3c) reveal an in-plane rotation of the long molecular axis relative to the chain direction, consistent with the formation of a quasi-square-planar binding pocket around the V centers that consists of two N of tetrazine units and two N of either pyridinyl or pyrimidinyl groups. The repeat distance is 6.5 Å ± 0.4 Å with the molecular axis oriented at a 55 ± 5° angle to the chain direction. Based on the repeat distance within the chain, the molecule orientation, and the known structure of the molecule, the V−N bond length

DOI: 10.1021/jacs.5b03706
J. Am. Chem. Soc. 2015, 137, 7898−7902

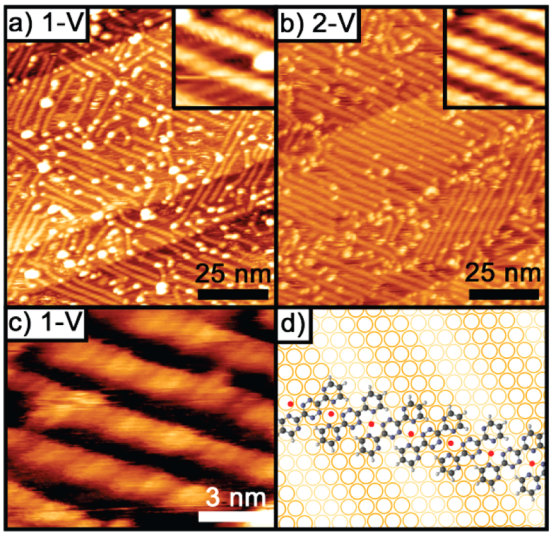

Figure 3. STM images of (a,c) **1**-V and (b) **2**-V chain structures on the reconstructed Au(100) surface. In (a,b), V metal was deposited to the sample first, followed by ligand, and then annealed at 200 °C. In (c), ligand **1** was deposited to the surface first, followed by V, and then annealed at 170 °C. The V:ligand ratio determined from XPS quantification is 1 in each case. The inset images in (a,b) have dimensions of 10 nm × 10 nm. (d) Schematic model of **2**-V chain structure. The **1**-V chain structure is identical.

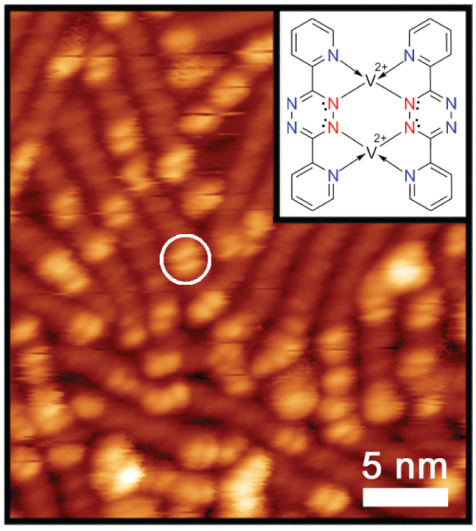

Figure 4. STM image and interpretative model of the second-layer **1**-V structure after annealing at 170 °C for 10 min, with total surface coverage exceeding one monolayer (XPS V:**1** ratio = 1; all V in +2 oxidation state). In the inset model, the red N atoms are amides (anionic) and the blue N atoms are imines (neutral) donors.

in these structures is determined to be 2−2.5 Å. The **1**-V and **2**-V chains are oriented at a 45 ± 5° angle to the Au reconstruction rows (insets of Figure 3a,b). The Au(100) surface spontaneously reconstructs to a quasi-hexagonal $c(26\times68)$ structure with a slight surface rumpling in rows that run in the [011] direction;[19,20] note that these reconstruction rows slightly affect the contrast variation along the chains in Figure 3c (compare to model in Figure 3d). The appearance and spacing of features along the chains are uniform in the STM measurements, which is consistent with all of the molecules in a given chain assuming the same orientation. The redox process is most efficient (less annealing required) if the ligand is deposited first and the metal second, but the opposite deposition order produces the same structure; i.e., addition of either ligand to already-formed V islands yields the same 1D metal−ligand polymer structure (Figure 3a,b; Figure S5 shows the V metal islands before ligand addition).

At higher coverage, second-layer growth initiates on top of the ends and defect sites of first-layer chains (Figure 4) for the **1**-V system. Second-layer growth already begins before the first layer is complete (Figure 3a), likely due to kinetic limitations in completing the first layer. Second-layer structures have an apparent elevation of 3−4 Å above the first-layer chains in the STM topography; that apparent height difference is consistent with a $\pi-\pi$ stacking distance,[29] but is large compared to the apparent height of the first layer above the surface (2−2.5 Å) and compared to other STM measurements of stacking of aromatic species.[29,30] In the initial stages of second-layer growth small discrete units that each appear as a pair of lobes are observed by STM measurements (white circle in Figure 4), each matching the size of a pair of molecules with a separation of 6.5 Å. (Note that these measurements were repeated in multiple experiments and the paired lobes are observed in various orientations to exclude the possibility of tip artifact.) With a partly filled second layer (Figure 4), XPS indicates a 1:1 ratio of **1**:V. In fitting the V peaks, width and position are indistinguishable from experiments with only first layer **1**-V complexes, indicating that all V (first and second layer) is in the +2 oxidation state. If we assume that the pairs contain V atoms, then the sample in Figure 4 should have 20% of surface V in the second-layer paired lobes, i.e., a quantity which should have an observable effect on the XPS spectra if those atoms were charge neutral. Second-layer growth can occur at any point along a first-layer chain, but by far most frequently occurs at the chain ends or defect sites.[31] It is possible that preferred growth on top of the terminal ligand or defect sites of first-layer chains may be related to a different chemical state of the first-layer ligand or metal at those positions, e.g., a −1 charge state of the terminal ligands compared to a −2 charge state of nonterminal ligands in the **1**-V polymer. The molecular structure drawing in Figure 4, which is consistent with the tendency toward forming two-molecule units, uses a feature of the pyridinyl substituent which is absent in the pyrimidinyl substituent: rotation of the pyridinyl inward provides an attractive site for a second metal, and simultaneously changes the reactivity character of the outside unit to one which does not propagate further growth. This feature is absent with the pyrimidinyl substituent, since its rings are two-fold symmetric. A similar structure is known to form in solution systems.[32]

■ CONCLUSION

We have shown that the molecular design of aromatic units pendant to tetrazine can alter the ligand redox character to an extent that is sufficient to achieve different oxidation states in coordinated V atoms. We have thus stabilized single-site V atoms in either a +2 or +3 oxidation state in 1D metal−ligand assemblies on a surface. The change in the ligand terminal functional groups from pyridinyl to pyrimidinyl functionalization increases the electron withdrawing action from the central tetrazine. The structures of the 1D polymers for either ligand have been shown to be virtually identical by high-resolution STM. In each case the repeat unit consists of a single molecule and single metal. Two tetrazine nitrogen atoms and two pyridinyl (in **1**-V) or pyrimidinyl (in **2**-V) nitrogen atoms are

DOI: 10.1021/jacs.5b03706
J. Am. Chem. Soc. 2015, 137, 7898−7902

bound to the cationic metals in a near-square-planar coordination geometry. The unbound pyrimidinyl N in **2**-V can accept some of the negative charge attendant to reduction, thus stabilizing the redox change. These experiments demonstrate the possibility of programming the oxidation state of single site transition metals at solid surfaces by coordinating ligand design. This strategy is common in homogeneous catalyst design and is very desirable for developing next-generation heterogeneous catalysts with higher levels of chemical selectivity, particularly for challenging problems in alkane oxidation and functionalization.

■ ASSOCIATED CONTENT

Supporting Information

Experimental details, STM images, XPS data, and analysis of the metal−ligand structures. The Supporting Information is available free of charge on the ACS Publications website at DOI: 10.1021/jacs.5b03706.

■ AUTHOR INFORMATION

Corresponding Authors

*caulton@indiana.edu

*tait@indiana.edu

Notes

The authors declare no competing financial interest.

■ ACKNOWLEDGMENTS

S.L.T. acknowledges support for this work from the Chemical Sciences, Geosciences and Biosciences Division, Office of Basic Energy Sciences, Office of Science, U.S. Department of Energy, Grant DE-FG02-12ER16351. K.G.C. acknowledges the Indiana University Office of Vice President for Research and the National Science Foundation, Grant CHE-1362127. D.S. and B.J.C. thank the Raymond Siedle Foundation for Fellowship funding.

■ REFERENCES

(1) Boscoboinik, J.; Kestell, J.; Garvey, M.; Weinert, M.; Tysoe, W. T. *Top. Catal.* **2011**, *54*, 20.

(2) Simard, G. L.; Steger, J. F.; Arnott, R. J.; Siegel, L. A. *Ind. Eng. Chem.* **1955**, *47*, 1424.

(3) Weng, W.; Davies, M.; Whiting, G.; Solsona, B.; Kiely, C. J.; Carley, A. F.; Taylor, S. H. *Phys. Chem. Chem. Phys.* **2011**, *13*, 17395.

(4) Gottfried, J. M.; Flechtner, K.; Kretschmann, A.; Lukasczyk, T.; Steinrück, H. P. *J. Am. Chem. Soc.* **2006**, *128*, 5644.

(5) Bai, Y.; Buchner, F.; Wendahl, M. T.; Kellner, I.; Bayer, A.; Steinrück, H. P.; Marbach, H.; Gottfried, J. M. *J. Phys. Chem. C* **2008**, *112*, 6087.

(6) Tait, S. L.; Wang, Y.; Costantini, G.; Lin, N.; Baraldi, A.; Esch, F.; Petaccia, L.; Lizzit, S.; Kern, K. *J. Am. Chem. Soc.* **2008**, *130*, 2108.

(7) Skomski, D.; Tempas, C. D.; Smith, K. A.; Tait, S. L. *J. Am. Chem. Soc.* **2014**, *136*, 9862.

(8) Skomski, D.; Tempas, C. D.; Bukowski, G. S.; Smith, K. A.; Tait, S. L. *J. Chem. Phys.* **2015**, *142*, 101913.

(9) Kaim, W. *Coord. Chem. Rev.* **2002**, *230*, 127.

(10) Arends, I. W. C. E.; Sheldon, R. A.; Wallau, M.; Schuchardt, U. *Angew. Chem., Int. Ed.* **1997**, *36*, 1144.

(11) Ramaswamy, A. V.; Sivasanker, S. *Catal. Lett.* **1993**, *22*, 239.

(12) Gupta, K. C.; Sutar, A. K. *Coord. Chem. Rev.* **2008**, *252*, 1420.

(13) Coates, G. W.; Hustad, P. D.; Reinartz, S. *Angew. Chem., Int. Ed.* **2002**, *41*, 2236.

(14) Hirao, T. *Encyclopedia of Inorganic Chemistry*; John Wiley & Sons, Ltd.: Chichester, England, 2006.

(15) Silversmit, G.; Depla, D.; Poelman, H.; Marin, G. B.; De Gryse, R. *J. Electron Spectrosc. Relat. Phenom.* **2004**, *135*, 167.

(16) Stepanow, S.; Strunskus, T.; Lingenfelder, M.; Dmitriev, A.; Spillmann, H.; Lin, N.; Barth, J. V.; Wöll, C.; Kern, K. *J. Phys. Chem. B* **2004**, *108*, 19392.

(17) Ge, Y.; Adler, H.; Theertham, A.; Kesmodel, L. L.; Tait, S. L. *Langmuir* **2010**, *26*, 16325.

(18) Horcas, I.; Fernández, R.; Gómez-Rodríguez, J. M.; Colchero, J.; Gómez-Herrero, J.; Baro, A. M. *Rev. Sci. Instrum.* **2007**, *78*, 013705.

(19) Van Hove, M. A.; Koestner, R. J.; Stair, P. C.; Bibérian, J. P.; Kesmodel, L. L.; Bartoš, I.; Somorjai, G. A. *Surf. Sci.* **1981**, *103*, 189.

(20) Van Hove, M. A.; Koestner, R. J.; Stair, P. C.; Bibérian, J. P.; Kesmodel, L. L.; Bartoš, I.; Somorjai, G. A. *Surf. Sci.* **1981**, *103*, 218.

(21) Kaim, W.; Fees, J. *Z. Naturforsch. B* **1995**, *50*, 123.

(22) Kasperkiewicz, J.; Kovacich, J. A.; Lichtman, D. *J. Electron Spectrosc. Relat. Phenom.* **1983**, *32*, 123.

(23) Woodruff, D. P.; Delchar, T. A. *Modern Techniques of Surface Science*, 2nd ed.; Cambridge University Press: Cambridge, UK, 1994.

(24) Eguchi, K.; Nakagawa, T.; Takagi, Y.; Yokoyama, T. *J. Phys. Chem. C* **2015**, *119*, 9805.

(25) Moulder, J. F.; Chastain, J. *Handbook of X-ray Photoelectron Spectroscopy: A Reference Book of Standard Spectra for Identification and Interpretation of XPS data*; Physical Electronics Division, Perkin-Elmer Corp.: Eden Prairie, MN, 1992.

(26) Hoang, T. K. A.; Webb, M. I.; Mai, H. V.; Hamaed, A.; Walsby, C. J.; Trudeau, M.; Antonelli, D. M. *J. Am. Chem. Soc.* **2010**, *132*, 11792.

(27) XPS reference data for the V(I) and V(II) charge states are rare. In vanadium oxides, the feature at 513.7 eV (which matches the value for **1**-V) is thought to correspond to vanadium(II) since a pure vanadium(I) oxide structure does not exist.

(28) The Au surface likely plays some role in affecting the final charge distribution of the system. Detailed theoretical studies, which are beyond the scope of this work, will be needed to fully address these questions. However, we note that the extent of redox observed spectroscopically here can be fully rationalized by in-plane charge transfer and known redox potentials of the employed ligands and metals. Indeed, in our studies so far of these and similar on-surface redox processes (refs 7 and 8), we have not yet observed significant deviations from solution-based redox behavior due to the surfaces, but perhaps other surfaces would play a more active role.

(29) Skomski, D.; Jo, J.; Tempas, C. D.; Kim, S.; Lee, D.; Tait, S. L. *Langmuir* **2014**, *30*, 10050.

(30) Chen, Q.; Rada, T.; McDowall, A.; Richardson, N. V. *Chem. Mater.* **2002**, *14*, 743.

(31) In a sampling of 47 first-layer chains in a 50 nm × 50 nm scan area with an average length of 14 ± 7 nm (corresponding to an average of 22 monomer units per chain and approximately 1000 total monomer units in all the chains), 83% (100/120) of the second-layer units were located at the end or at defects sites (points where chains bend) along the chains.

(32) Constable, E. C.; Housecroft, C. E.; Kariuki, B. A.; Kelly, N.; Smith, C. B. *C. R. Chim.* **2002**, *5*, 425.

DOI: 10.1021/jacs.5b03706
J. Am. Chem. Soc. 2015, 137, 7898−7902